

Learned Digital Subtraction Angiography (Deep DSA): Method and Application to Lower Extremities

P-1.20

Elias Eulig^{1,}, Joscha Maier¹, Michael Knaup¹, Thomas Koenig², Klaus Hörndl², and Marc Kachelrieß¹*

¹ German Cancer Research Center (DKFZ), Heidelberg, Germany

² Ziehm Imaging GmbH, Nuremberg, Germany

dkfz.

**GERMAN
CANCER RESEARCH CENTER
IN THE HELMHOLTZ ASSOCIATION**

Research for a Life without Cancer

**Send correspondence to Elias Eulig (elias.eulig@dkfz.de)*

Abstract

Digital Subtraction Angiography aims at selectively displaying vessels by subtracting an unenhanced mask image from a contrast-enhanced fluoroscopic image. This strategy requires the data to be static, i.e. to be acquired without patient or C-arm motion, making conventional DSA infeasible for dynamic acquisition protocols such as bolus injection chases. Deep DSA utilizes a convolutional neural network to predict DSA-like images directly from their corresponding fluoroscopic x-ray images. Here, we demonstrate the potential of this approach for static and dynamic fluoroscopic acquisitions of the lower extremities. For cases where a conventional DSA is feasible we examine very small deviations and observe predictions for the bolus chase studies of similar visual impression as with conventional DSA.

Introduction

Digital subtraction angiography (DSA)¹ exams are performed by acquiring a series of x-ray images using a C-arm system while injecting contrast media into the vessels. The contrast media alters the radiodensity of the vessels, resulting in a clear contrast with respect to the surrounding tissue present in the x-ray image. To selectively display these vessels, a mask image acquired prior to contrast agent injection is subtracted from all subsequent frames . One major drawback of this technique is its limitation to reasonably static data, thus making applications dynamic acquisition protocols such as bolus chase studies² of the lower extremities impractical.

Predicting the DSA from a single contrast-enhanced x-ray image can be formulated as an image-translation problem, making convolutional neural networks (CNNs) likely to be capable of overcoming the mentioned downside of conventional DSA. Deep DSA³ utilizes a CNN in order to directly learn DSA-like images from the fluoroscopy image without the need to acquire a mask image beforehand. Here, we apply Deep DSA to data of clinical relevance, namely both static and dynamic fluoroscopic x-ray images from the lower extremities.

Methods

Training Data: All training data were acquired using various models of C-arms manufactured by Ziehm Imaging with Iodine as contrast agent. The training data consist of 60 cases from the lower extremities: 57 being static data (without C-arm motion) and 3 being dynamic bolus chase studies where the C-arm is moved during the acquisition. 48 static datasets were used for training and 12 datasets, including the 3 bolus chase studies, were used for quantitative and qualitative validation.

Training Details: In order for the network to simultaneously preserve the fine details present in the vessels and capture long-range dependencies necessary to differentiate the vessels from surrounding structures, we used an encoder-decoder structure with concatenated skip-connections between the contracting and expanding part, similar to a U-Net⁴ (Fig. 1).

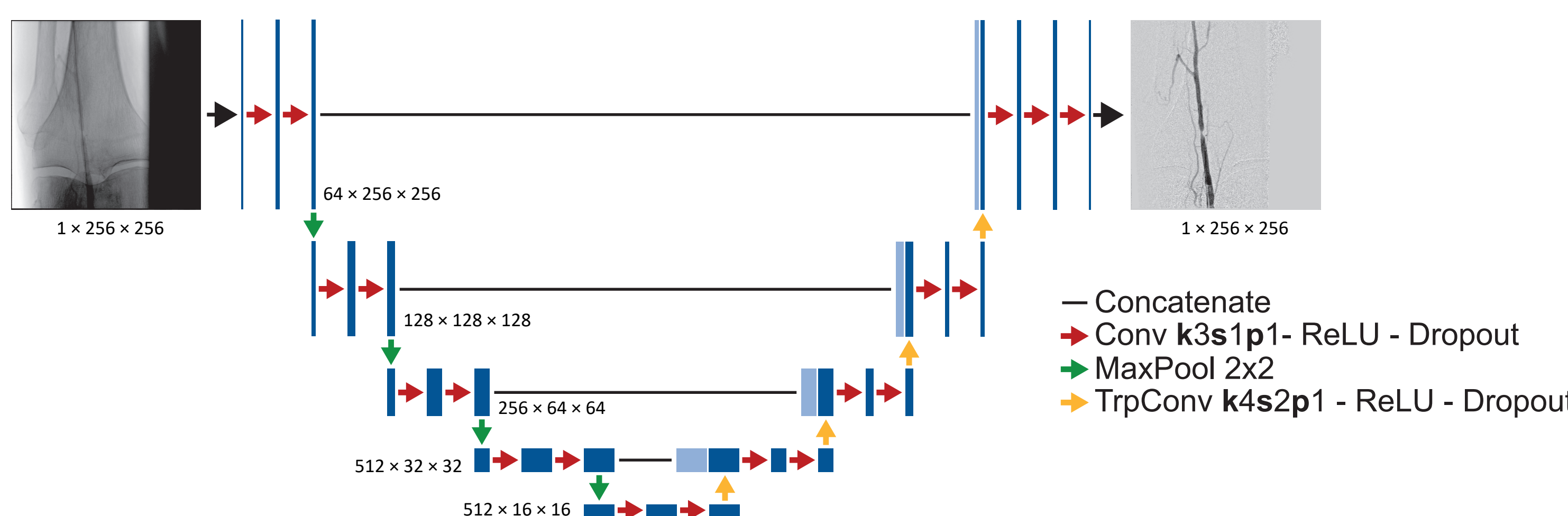


Figure 1. Structure of the Deep DSA network resembling a U-Net. Downsampling is performed using max-pooling and upsampling using transposed convolutions. We employ ReLUs as nonlinearities and spatial dropout to help the network generalize.

To further generalize of the network we used spatial-dropout⁵ layers and data augmentation including random flips, rotations, shearing, scaling, blurring and piecewise affine transformations. Training was performed patch-wise and the \mathcal{L}_1 loss between output and ground truth was minimized using the Adam optimizer.

Results & Discussion

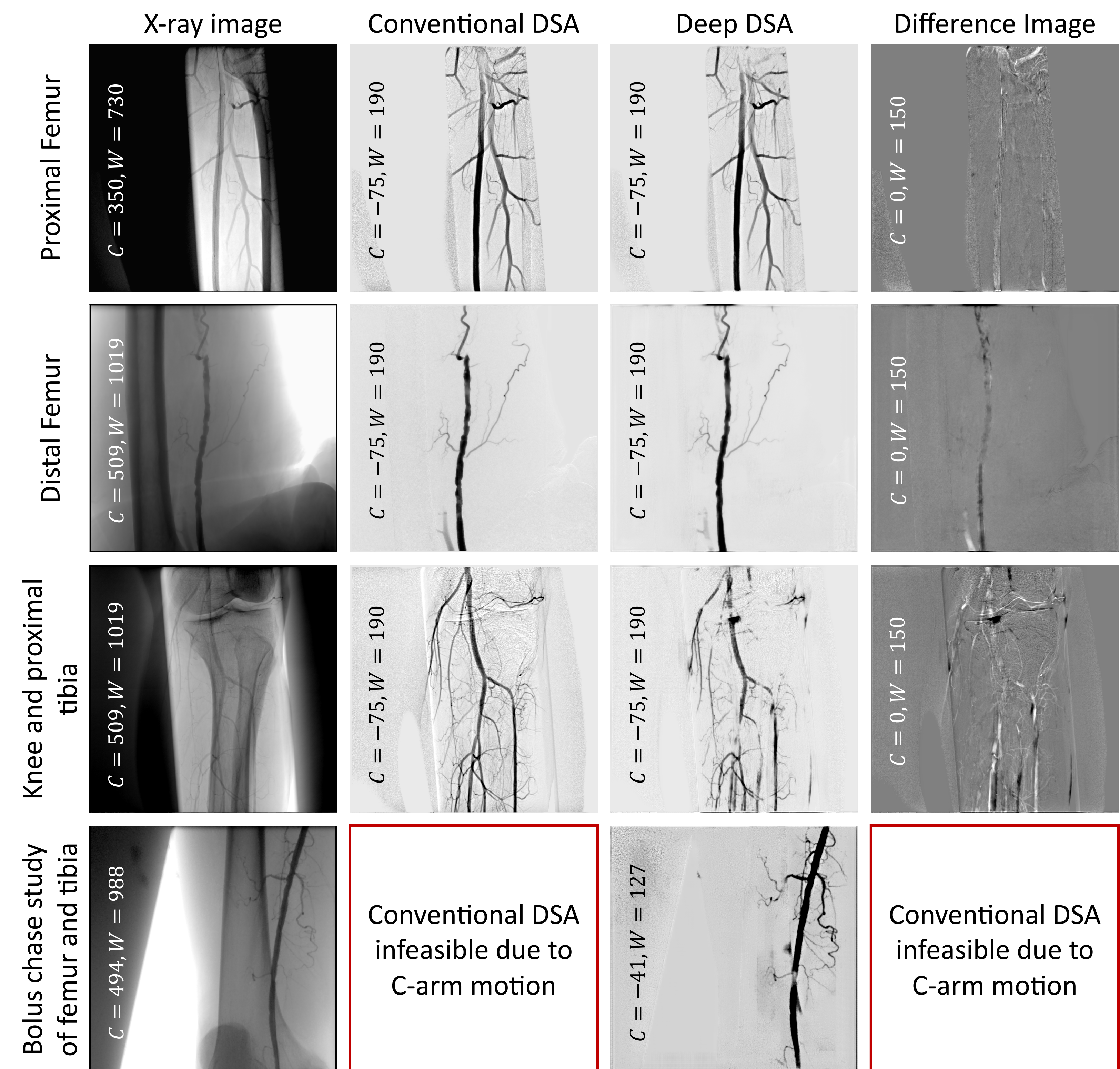


Figure 2. X-ray image, conventional DSA, Deep DSA and difference image (Deep DSA–Conventional DSA) for four angiographic exams: Proximal femur, distal femur, knee and proximal tibia and bolus chase study of the femur and tibia. Note, that for the bolus chase study conventional DSA is infeasible and thus no direct comparison between Deep DSA and conventional DSA can be made.

We observe that Deep DSA output images are generally very similar in appearance to the conventional DSA for all three static exams (Fig. 2). For the bolus chase, where there is no conventional DSA available, the Deep DSA output resembles a conventional DSA in its visual impression. We notice that Deep DSA fails to adequately visualize several small vessels in the study of the knee and proximal tibia, which is most likely due to a lack of training data for those structures and is intended to be further investigated and ultimately eliminated in future studies.

References

- [1] Kruger, R. A., Mistretta, C. A., Houk, T. L., Riederer, S. J., Shaw, C. G., Goodsitt, M. M., Crummy, A. B., Zwiebel, W., Lancaster, J. C., Rowe, G. G., and Flemming, D., "Computerized Fluoroscopy in Real Time for Noninvasive Visualization of the Cardiovascular System," *Radiology* 130(1), 49–57 (1979).
 - [2] Jurriaans, E. and Wells, I. P., "Bolus chasing: a new technique in peripheral arteriography," *Clinical radiology* 48(3), 182–185 (1993).
 - [3] Eulig, E., Maier, J., Knaup, M., Koenig, T., Hörndl, K., and Kachelrieß, M., "Deep DSA (DDSA): Learning mask-free digital subtraction angiography for static and dynamic acquisitions protocols using a deep convolutional neural network," *ECR 2019 Book of Abstracts, Insights into Imaging* 10 Suppl. 1 (B- 0909), 379 (2019).
 - [4] Ronneberger, O., Fischer, P., and Brox, T., "U-Net: Convolutional networks for biomedical image segmentation," *Medical Image Computing and Computer-Assisted Intervention* 9351, 234–241 (2015).
 - [5] Tompson, J., Goroshin, R., Jain, A., LeCun, Y., and Bregler, C., "Efficient object localization using convolutional networks," *Proceedings of the IEEE Conference on Computer Vision and Pattern Recognition*, 648–656 (2015).